Sedimentology (2003) **50,** 1221–1229 doi: 10.1046/j.1365-3091.2003.00602.x

Kaolinitic meniscus bridges as an indicator of early diagenesis in Nubian sandstones, Sinai, Egypt

XAVIER DU BERNARD and ELISABETH CARRIO-SCHAFFHAUSER
Laboratoire de Géophysique Interne et Tectonophysique (UMR 5559), BP 53X, 38041 Grenoble cedex 9, France (E-mail: xduberna@obs.ujf-grenoble.fr)

ABSTRACT

Characteristic meniscus geometries formed by kaolinitic infiltration are observed in Nubian sandstones collected on the western coast of the Sinai Peninsula (Egypt). Based on petrographic and scanning electron microscope (SEM) observations, the kaolinite forming the menisci consists of mixed-size discrete platelets that gather into the corners around the framework grain-to-grain contacts. Specifically, the internal fabric of menisci indicates a general organizing trend from (1) the centre, where the platelets coat the framework grains; (2) to the peripheral zone, where they are oriented tangentially to grain surfaces; (3) to the pore linings with curvatures that are consistent with theoretical considerations of air–water interfaces. This typical arrangement suggests a detrital origin of kaolinite platelets by mechanical infiltration into sediments lying above the tablewater, in vadose conditions. This type of clay cementation occurring during early diagenesis can prevent (delay) deep burial diagenetic processes and therefore preserve excellent reservoir properties.

Keywords clay minerals, kaolinite, Nubian sandstone, sandstone diagenesis.

INTRODUCTION

Early diagenesis of sediment can occur shortly after deposition. Depending on depositional environment, the early lithification (i.e. the first developed bonding agent) occurs as carbonate precipitation or particle infiltration that links framework grains by forming meniscus bridges. Such grain-to-grain bridges grow preferentially in the corners of pore space close to grain contacts (Dunham, 1971). Specifically, by developing in conformity to the water–air interface (the meniscus) as a result of differential capillarity pressures, these cements or infiltrating material are assumed to be related to vadose environments (Dunham, 1971).

The meniscus geometry forming pore-rounding habit has been described frequently in modern sedimentary environments where carbonate precipitation produces beachrocks from carbonate sands (Meyers, 1987; Hillgärtner *et al.*, 2001). These types of precipitated meniscus cements consist mainly of crypto- to microcrystalline calcite or aragonite that display filaments, which generally grow perpendicular to grain rim (Miller, 1988; Rao *et al.*, 1994; Hillgärtner *et al.*, 2001). In contrast, precipitated menisci of goethitic-ferruginous material have been reported for a lateritic profile in basalt (Horváth *et al.*, 1999).

Several studies have also dealt with the meniscus shape displayed by mechanically infiltrated clay particles in clastic sediments (Walker, 1976; Kessler, 1978; Meyers, 1987; Matlack *et al.*, 1989; Moraes & De Ros, 1990). Owing to the micrometre-scale size of particles, the detrital clays are transported along connected pores by fluids circulating between skeleton grains (Walker, 1976). During a drying period, the detrital clays gather where the capillarity pressure preserves fluids. Therefore, the accumulated clays exhibit grain coatings and meniscus-shaped bridges linking neighbouring grains. Thus, the meniscus cements typically indicate vadose conditions where pore spaces are not permanently saturated, i.e. water-table level fluctuates (Walker, 1976; Matlack *et al.*, 1989; Moraes & De Ros, 1990;

Horváth *et al.*, 1999). The laboratory experiments reveal that the major parameters controlling the amount of accumulated clays are framework grain size and shape, as well as concentration and composition of clay particles (Matlack *et al.*, 1989).

Nevertheless, none of the previous studies has focused on the internal structure and the exact shape of the meniscus, nor closely described the mechanisms of particle accumulation. Based on microscopic observations, the current study suggests that a progressive organization of clay platelets occurs with sequential accumulation.

The aim of this study is to describe the structure of menisci in order to understand the processes of concentration, i.e. the modes of localization and development of infiltration. An important application is to constrain better the evolution of porosity and permeability, which determine the evolution of fluid circulation during early diagenesis. Moreover, the nature and amount of cement or infiltration are important parameters controlling physical properties of sandstones. Therefore, by characterizing the geometry of clay accumulation better, it may be possible to constrain pore space evolution and, consequently, reservoir properties during diagenetic processes. The Nubian sandstone provides an ideal formation in which to study meniscus fabric because of the large porosity and single kaolinitic cementation stage, which are preserved because of limited burial.

GEOLOGICAL SETTING

The Nubian sandstones constitute the first deposits of the prerift sediments in the Neogene Suez Rift (Garfunkel & Bartov, 1977). They were deposited on a cratonic domain from the Cambrian to the Cretaceous. In the western coast of the Sinai Peninsula (east border of Suez Gulf), this mainly sandy formation is up to 600 m thick (Robson, 1971) and comprises mostly continental deposits (Schütz, 1994). In the study area (Fig. 1), these sediments, predominantly fluvial (Said, 1962), show relatively little variation in depositional environment, except for some thin layers of shallow-marine sediments that were deposited during the Cambrian, Permian–Triassic and Jurassic periods (Fig. 2). Numerous sedimentary breaks with or without well-developed erosion surfaces are recorded, in particular at the base of Carboniferous, Triassic and Lower Cretaceous strata. A major Cenomanian transgression resulted in prerift marine formations that conformably cover the Nubian sandstones and comprise a 500–1000 m thick Cretaceous to Eocene succession (Schütz, 1994). The Cretaceous to Eocene marine units, much more shaly and calcareous, are overlain by synrift conglomerates and evaporite series in the e of the trough. The remarkable absence of significant angular discordance within the prerift sedimentary record indicates little tectonic activity before

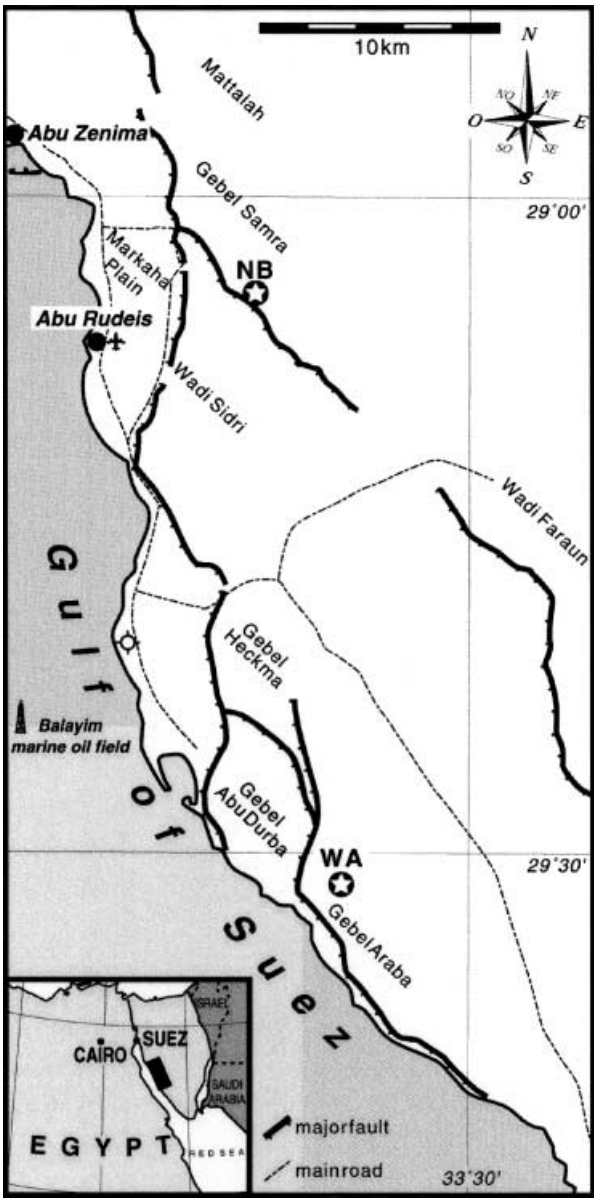

Fig. 1. Simplified structural map of the study area located on the eastern border of the Suez Rift (modified from the Sinai Geological Map 1:500 000 by Eyal *et al.*, 1980). White stars indicate the location of the two outcrops where samples were collected: Wadi Araba (WA) and Naqb Budra (NB).

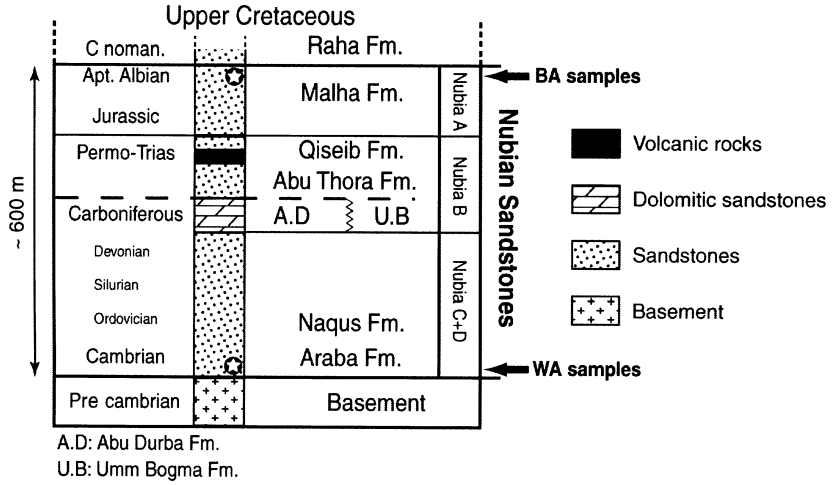

Fig. 2. Schematic stratigraphic column of the Nubian sandstones in the study area (modified from Schütz, 1994). White stars indicate the stratigraphic position of the collected samples: Wadi Araba (WA) and Naqb Budra (NB).

the rifting phase, which began in early Miocene time (23·5 My) (Garfunkel & Bartov, 1977; Chénet & Letouzey, 1983). Hence, on the border of the Suez rift, shallow burial and associated limited diagenesis (i.e. little compaction and precipitation) of the Nubian sandstones have resulted in a friable high-porosity material.

MICROTEXTURES OF INFILTRATED KAOLINITIC PARTICLES

Sample collection and preparation

All the collected samples come from two outcrops located at the border of the Suez rift, i.e. in areas with little or no synrift deposition, which implies limited burial. Samples were taken at the bottom and the top of the Nubian sandstone deposits, at Wadi Araba (WA) and Naqb Budra (BA) outcrops respectively (Fig. 2).

Optical and scanning electronic microscope (SEM; backscattered) observations were made in polished thin sections after blue epoxy impregnation under vacuum. For secondary electron SEM analyses, small chips of samples were coated with gold. In addition, sample fragments were gently ground and ultrasonically disaggregated before the separation of the < 2 μm size fraction. This size fractionation aimed at minimizing the contribution of quartz, while keeping the whole clay fraction, with the size of clay platelets being > 2–3 μm as observed with SEM. This clay separate was finally freeze dried and randomly oriented for X-ray diffraction analysis using a Siemens D5000 diffractometer, equipped with a Kevex Si(Li) solid-state detector, and CuKα1+2 radiation.

Petrographic microscopy and X-ray mineralogy

Optical microscope observations revealed that the Nubian sandstone samples represent a medium-grained quartz arenite, which is composed mainly of well-rounded and well-sorted quartz grains (Fig. 3A). Based on image analysis, the long axis of the best fitting ellipse was estimated for more than 250 grains. Using the Moment formulae given by Pettijohn *et al.* (1972), the calculation in Phi (Φ) units gives a mean size of 1·85 (sorting = 0·47) and 2·26 (sorting = 0·37) for samples from Naqb Budra and Wadi Araba respectively. Quartz overgrowths and concavo-convex contacts are rare, indicating few pressure solution effects.

Two modes of kaolinite occurrence were observed. (1) The cement is mainly formed by micrometre-scale clay bridges linking adjacent quartz grains (Fig. 3B). The preferential accumulation of clay particles close to the contact point results in a meniscus geometry producing a rounded shape for preserved pores. These clay accumulations show a typical brown colour that differs from the usual colour of pure kaolinite. Spectral analyses from SEM reveal iron and titanium contents. (2) Lighter authigenic kaolinite probably recrystallized from previous detrital particles totally fills some pores, as observed in other porous sandstones (Wilson & Pittman, 1977). These clots of authigenic kaolinite display some well-developed booklets formed by pseudohexagonal flakes of 10 μm diameter, as described for Nubian sandstones outcropping in the Western Desert (Egypt) (Hilmy & Hussein, 1980; Abu-Zeid, 1982) (Fig. 3C).

The XRD diffractograms (Fig. 4) indicate the absence of a peak at $\approx 4{\cdot}26$ Å, which confirms the

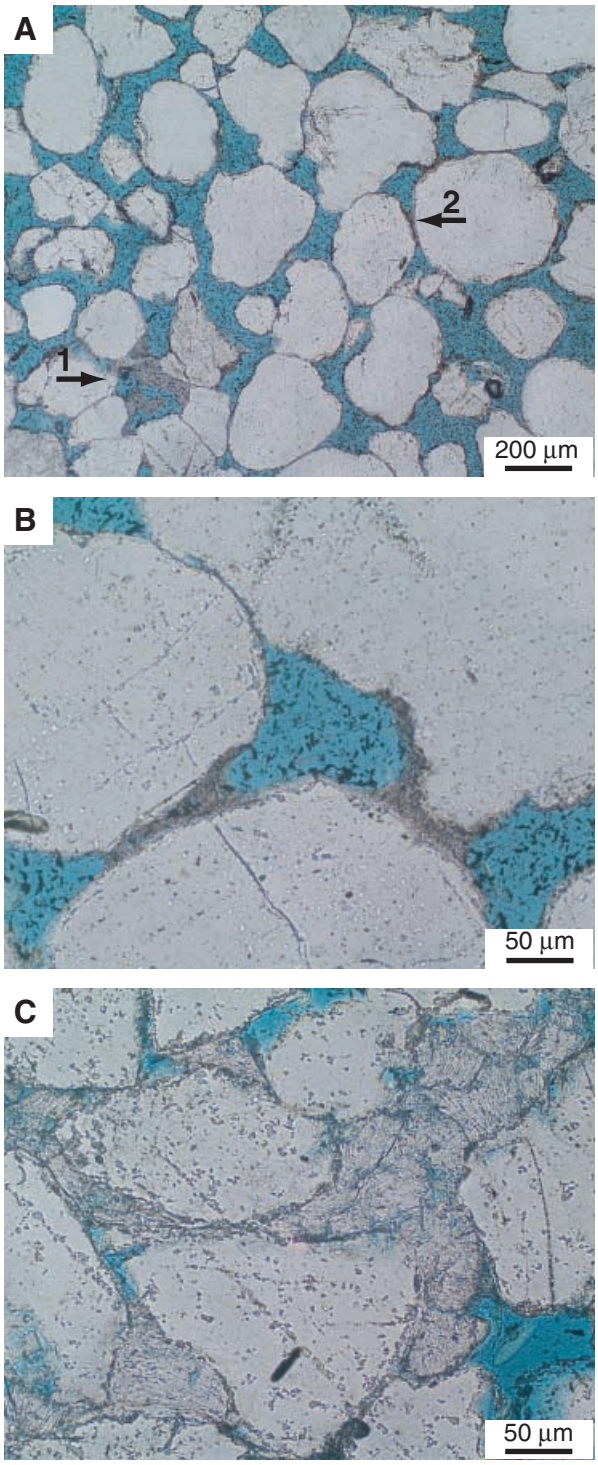

Fig. 3. Photomicrographs (plain light) of Nubian sandstones from Naqb Budra outcrop: the quartz grains appear white and the injected epoxy resin filling pores is blue. (A) Overview showing the medium-grained quartz arenite, which is composed mainly of well-rounded and sorted quartz grains. Authigenic kaolinite partially fills some pores (arrow 1). Large menisci of micrometre-scale detrital kaolinite platelets cementing the framework quartz grains are visible from the brown colour of iron oxides (arrow 2). (B) Close-up view of meniscus cement. The kaolinite platelets are concentrated near the quartz grain contacts. These kaolinite accumulations feature a meniscus geometry that results in a rounded shape for preserved pores. (C) Authigenic kaolinite probably recrystallized from detrital particle fills displaying some well-developed booklets. From the cross-section view, each plate of kaolinite is at least < 25 microns.

actual removal of quartz in the fine-grained fraction in which feldspar is also absent. In addition, the absence of the 4·26 Å peak supports the overwhelming presence of kaolinite, with respect to dickite, in the sample. This is confirmed by the positions of the two peaks at 4·475 and 4·366 Å, by the presence of two doublets, rather than single peaks, at 4·186–4·139 Å and 3·847–3·745 Å (Drits & Tchoubar, 1990) and over the 35–40°2ΘCuKα range (data not shown). Consequently, the fine fraction of the samples is exclusively formed by kaolinite.

Scanning electron microscopy (SEM)

SEM observations focus on the cemented grain-to-grain contacts to describe the geometry of kaolinite menisci (Fig. 5A). Around the point contacts, kaolinite particles form a coating deposited on the surface of framework detrital grains (Fig. 5A and B). In cross-section, the curvature of menisci can be characterized by a tangent circle as displayed in Figs 5B and C. In Fig. 5C and D, close-up views indicate that the menisci are formed by accumulations of kaolinite platelets, with sizes varying from 1 micron to several microns. The first deposited detrital kaolinite platelets exhibit a preferred orientation with the *c*-axis perpendicular to the detrital grain surface (face-to-face contact) (Fig. 5D). In the centre of the meniscus, where the distance between detrital grains is minimal, kaolinite platelets are more randomly oriented and locally arranged perpendicular to the previous platelets coating grains (edge-to-face contact). The external curved part of the meniscus (i.e. the interface between cement and pore) consists of kaolinite platelets organized tangentially to the regular curvature of the pore (Fig. 5D). Consequently, there is a general organizing trend from the centre to the external part of the meniscus that is assumed to be related to mechanical infiltration into sediments lying above the water table in vadose conditions.

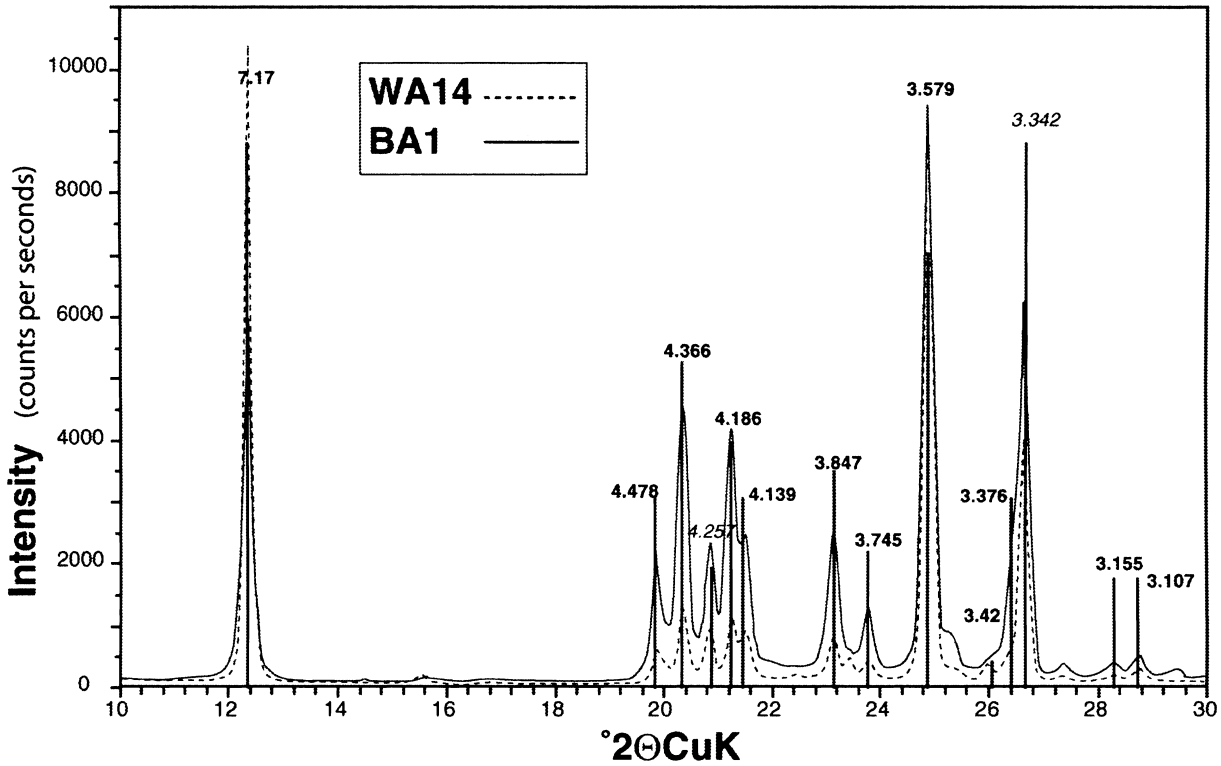

Fig. 4. XRD diffractogram of < 2 μm fraction extracted from Nubian sandstones. The peak values of samples from WA (dashed curve) and NB (continuous curve) fit adequately with the spectrum of the quartz (oblique values and dashed lines) and kaolin polytype (bold values and plain lines). The quartz probably corresponds to extra fine particles trapped and associated with kaolinite platelets within menisci.

DEVELOPMENT OF KAOLINITE BRIDGES

Kaolinite occurrence and timing of infiltration

During the early Palaeozoic until the pre-Upper Cretaceous, subaerial exposure surfaces are well known in north-east Africa (Schwarz & Germann, 1999). The alteration of cratonic basement made up by granitic, gneissic and siliciclastic rocks led to the formation of deep weathered materials and secondary accumulations formed by alluvial placers with sedimentary kaolinite and quartz. Microscopic observations reveal that most of the point contacts of quartz grains are surrounded by menisci formed by kaolinite platelets. In contrast, the lack of both planar contacts surrounded by kaolinite platelets and preferential grain orientation implies no grain rearrangement before infiltration timing. Therefore, the detrital platelets of kaolinite are deduced to infiltrate just after deposition as there is no evidence of compaction before infiltration. Moreover, the light patches of authigenic kaolinite post-date the menisci formed by rust-coloured platelets of detrital kaolinite. The rust colour probably indicates the presence of iron oxide in the clay mineral lattice in superficial oxidizing conditions, whereas the light colour corresponds to pure kaolinite developed in reducing conditions. Because of this relative chronology, the menisci are assumed to form just after deposition, i.e. during subsurface diagenesis, whereas the patches of authigenic kaolinite are assumed to develop with burial diagenesis.

Meniscus geometry and mechanisms of clay accumulation

The clay accumulations at the point contacts describe a meniscus shape similar to the pendular rings formed by the air–water interfaces in drained media, which have been exhaustively studied theoretically (Smith, 1933; Rose, 1958; Orr *et al.*, 1975; Gvirtzman & Roberts, 1991). In two dimensions, our observations indicating a circular shape for the menisci (see dashed circles in Fig. 5B) are consistent with the predicted constant curvature of the interfacial surface between air and water (i.e. the meniscus). The meniscus geometry requires minimum surface energy (Smith, 1933) and can be approximated as

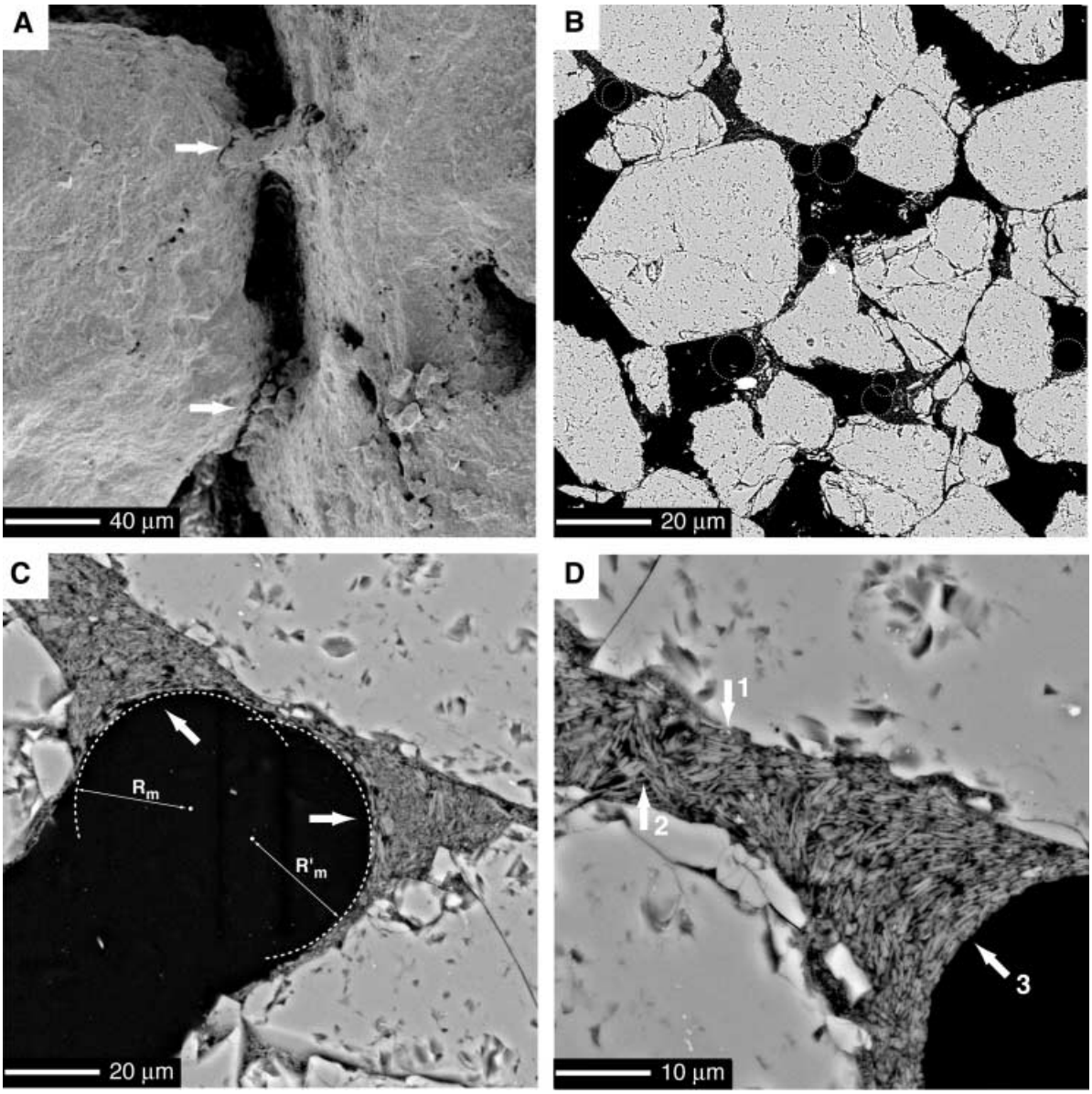

Fig. 5. SEM pictures of Nubian sandstones from Naqb Budra outcrop. (A) Secondary electron image showing clay bridges (white arrows) linking quartz grains. Owing to weak compaction, some quartz grains are not quite in contact; in these cases, the kaolinite bridges correspond to the liquid bridges that can persist after draining. (B) Backscattered image of sandstone overview. The quartz grains appear light grey, the kaolinite dark grey, and the injected epoxy resin filling pores is black. White dashed circles are overprinted to characterize the meniscus geometry. Note that just two quartz grains exhibit syntaxial overgrowths. (C) Backscattered image of meniscus formed by detrital kaolinite platelets (white arrows). White dashed arcs of circle (R_m and R_m' radii) are overprinted to characterize the meniscus geometry with constant curvature. (D) Close-up view of a detrital kaolinite meniscus. The size of kaolinite platelets varies from 1 to 5 microns. The first platelets deposited exhibit a preferred orientation with the elongated side parallel to the quartz grain surface (face-to-face contact) (arrow 1). In the centre of the meniscus where the distance between the two faces of quartz grains is minimal, kaolinite platelets are more randomly oriented and locally arranged perpendicular to the previous platelets coating grains (edge-to-face contact) (arrow 2). The external curved part of the meniscus consists of kaolinite platelets organized tangentially to the curvature of pore linings (arrow 3).

a circular arc of revolution tangential to the spheres (i.e. the detrital grains) (Rose, 1958). By considering cubic packing in two dimensions (Fig. 6), the radius (R_m) of the meniscus that forms between two spherical grains under equilibrium is given by $R_m = R_g \frac{1-\cos\varphi}{\cos(\varphi+\theta)}$, where R_g is the common radius of the contacting grains, θ the contact angle between water and grains and ϕ the

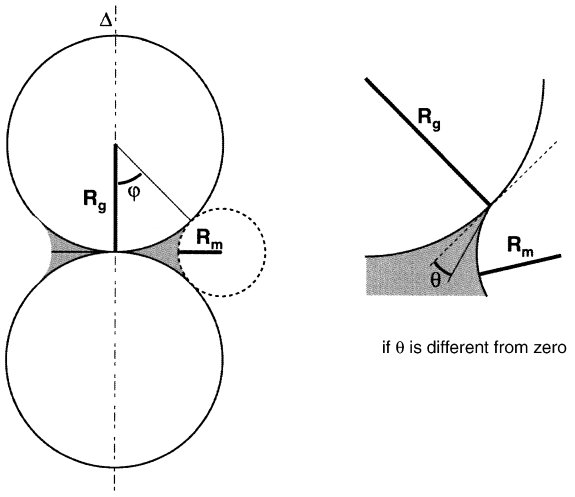

Fig. 6. Cross-section through the e of a meniscus (displayed in grey) between two identical spheres (*Rg* is the radius) in cubic arrangement. The radii R_m define the curvature of the interface between air and water and ϕ the 'water content index angle'. If the contact angle θ is not equal to zero, the circle of radius R_m is not tangential to the circle of radius R_g. See text for detailed geometry description.

'water content index angle' (Melrose, 1965; Likos & Lu, 2002).

Detrital clay platelets that are in suspension in flowing water circulate into the freshly deposited sand. During the drying periods, as water is being drained, clay platelets gather into the zones where the capillary pressure preserves fluids, i.e. within the water film surrounding skeleton grains and, in particular, close to grain contacts where the water–air interface exhibits a meniscus geometry. Consequently, the first platelets that deposit on the detrital grain surfaces exhibit a face-to-face arrangement resulting from both the possible thinness of the film and, more probably, the interactions with detrital grains. This suggested coating during the desiccation phases is supported by calculations and experiments on synthetic binary mixtures of sand and clays (Fies & Bruand, 1998). In the centre of menisci, the next platelets are not systematically deposited in conformity with the first ones because of a relatively large water volume. The platelets then appear to be randomly oriented with edge-to-face contacts. This local disorganization results in an intragranular porosity. When the narrow and angular part of the pore corner is totally filled with disorganized platelets, new platelets are deposited progressively in conformity with the air–water interface until their orientation is tangential to the meniscus boundary. These last deposited platelets are characterized by a face-to-face organization. The experiments on a synthetic aggregate of clays and quartz sand subjected to wetting and drying cycles suggest that the clay particles become oriented into more face-to-face associations and the sand–clay interactions increase with the number of cycles (Fies & Bruand, 1998). Hence, the well-organized platelets that are observed miming the air–water interface would be the result of several variations in the water table. Multiple phases of deposition are not inconsistent with the described model for meniscus cementation formed by detrital platelets of clays. Actually, as the molecular forces prevent the complete drainage of water from the void space and as the ionic forces and the tangle disposition prevent total leaching, the kaolinite platelets stay in place and accumulate progressively. As suggested by Singer *et al.* (1992) from their experiment on synthetic sand–clay aggregates, kaolinite may be stabilized by H bonds between O atoms in the tetrahedral sheet of one layer and OH groups in the octahedral sheet of the adjacent layer. Although the water is agitated, these bonds remain strong, and the kaolinite neither swells nor disperses. Finally, the brown colour of menisci probably indicates the presence of iron oxide in the clay mineral lattice, resulting from repeated bathing of subsurface waters as suggested by Walker (1976) for the Red Beds, and that strengthens the particle bonds.

Preservation of clay structure and consequences

Supported by XRD analysis, the sole presence of kaolinite indicates that the kaolinite-to-dickite transformation has not begun, indicating limited burial (< 2500 m; Beaufort *et al.*, 1998; Lanson *et al.*, 2002). The lack of mechanical and chemical compaction as a result of limited burial, combined with the probable absence of organic acid-rich fluid circulations, contributes to the stability of kaolinite.

According to Bernabé *et al.* (1992), the cement, even in very small quantity, significantly increases the strength of granular material, in particular when it is located at the grain-to-grain contacts. Hence, the clay cementation occurring in meniscus geometry is sufficient to increase the overall strength of sandstone and preclude the rearrangement of detrital quartz grains by rotation and sliding. Moreover, clay coatings that can be locally well developed are considered to be important in inhibiting cementation on detrital quartz because they reduce the surface area available for

precipitation (Renard *et al.*, 2001). Thus, clay cementation can slow mechanical and chemical compaction, and can inhibit quartz cementation, thus preserving primary porosity in hydrocarbon reservoirs. This is confirmed by the equal porosity for samples collected from the two studied outcrops (WA and BA) even though there is an approximate 600 m difference in burial.

ACKNOWLEDGEMENTS

This research was supported by IFP through a convention with LGIT, Joseph Fourier University (Grenoble). We are grateful to I. Moretti and B. Colletta for their confidence and help in the field for sample collection. F. Claret is greatly thanked for performing the XR analysis. We thank A. Arnaud and B. Lanson for critical discussions and comments on these results. We would like to thank the two reviewers, Drs Ramseyer and Houseknecht, for their constructive reviews, which have greatly improved the second draft of the manuscript. Thanks are also due to the Associate Editor, Dr Spötl, whose patience and insightful suggestions have led to a new concise revised version.

REFERENCES

Abu-Zeid, M.M. (1982) Authigenic clay minerals in the Nubia Sandstone of Kharga Oasis (Western Desert, Egypt) as revealed by scanning electron microscopy. *Neues Jb. Mineral. Abh.*, **144,** 214–229.

Beaufort, D., Cassagnabère, A., Petit, S., Lanson, B., Berger, G., Lacharpagne, J.C. and **Johansen, H.** (1998) Kaolinite-to-dickite conversion series in sandstone reservoirs. *Clay Mineral.*, **33,** 297–316.

Bernabé, Y., Fryer, D.T. and **Hayes, J.A.** (1992) The effect of cement on the strength of granular rocks. *Geophys. Res. Lett.*, **19,** 1511–1514.

Chénet, P.Y. and **Letouzey, J.** (1983) Tectonique de la zone comprise entre Abu Durba et Gebel Mezzazat (Sinaï, Egypte) dans le contexte de l'évolution du Rift de Suez. *Bull. Centres Rech. Explor.-Prod. Elf-Aquitaine*, **7,** 201–215.

Drits, V.A. and **Tchoubar, C.** (1990) *X-Ray Diffraction by Disordered Lamellar Structures.* Springer-Verlag, Berlin, 371 pp.

Dunham, R.J. (1971) Meniscus cement. In: Carbonates Cements (Ed. O.P. Bricer, Vol. 19, pp. 297–300. The Johns Hopkins University Studies in Geology, Baltimore, MD.

Eyal, M., Bartov, Y., Shimron, A.E. and **Bentor, Y.K.** (1980) *Sinai – Geological Map.* Survey of Israel.

Fies, J.C. and **Bruand, A.** (1998) Particle packing and organization of the textural porosity in clay-silt-sand mixtures. *Eur. J. Soil Sci.*, **49,** 557–567.

Garfunkel, Z. and **Bartov, Y.** (1977) The tectonics of Suez Rift. *Geol. Surv. Israel Bull.*, **71**.

Gvirtzman, H. and **Roberts, P.V.** (1991) Pore scale spatial analysis of two immiscible fluids in porous media. *Water Resour. Res.*, **27,** 1165–1176.

Hillgärtner, H., Dupraz, C. and **Hug, W.** (2001) Microbially induced cementation of carbonate sands: are micritic meniscus cement good indicators of vadose diagenesis? *Sedimentology*, **48,** 117–131.

Hilmy, M.E. and **Hussein, S.A.** (1980) Diagenesis of Nubia Sandstone as revealed by scanning electron microscopy. *Egypt. J. Geol.*, **22,** 87–101.

Horváth, Z., Varga, B. and **Mindszenty, A.** (1999) Micromorphological and chemical complexities of a lateritic profile from basalt (Jos Plateau, Central Nigeria). *Chem. Geol.*, **170,** 81–93.

Kessler, L.G. (1978) Diagenetic sequence in ancient sandstones deposited under desert climatic conditions. *J. Geol. Soc. London*, **135,** 41–49.

Lanson, B., Beaufort, D., Berger, G., Bauer, A., Cassagnabère, A. and **Meunier, A.** (2002) Authigenic kaolin and illitic minerals during burial diagenesis of sandstones: a review. *Clay Mineral.*, **37,** 1–22.

Likos, W.J. and **Lu, N.** (2002) Hysteresis of capillary cohesion in unsaturated soils. In: *15th ASCE Engineering Mechanics Conference*, New York.

Matlack, K.S., Houseknecht, D.W. and **Applin, K.** (1989) Emplacements of clay into sand by infiltration. *J. Sed. Petrol.*, **59,** 77–87.

Melrose, J.C. (1965) Wettability as related to capillary action in porous media. *Soc. Petrol. Eng. J.*, **5,** 259–271.

Meyers, J.H. (1987) Marine vadose beachrock cementation by cryptocrystalline magnesian calcite – Maui, Hawaii. *J. Sed. Petrol.*, **57,** 558–570.

Miller, J. (1988) Cathodoluminescence microscopy. In: *Techniques in Sedimentology* (Ed. M. Tucker), pp. 174–190. Blackwell Scientific Publications, Oxford.

Moraes, M.A.S. and **De Ros, L.F.** (1990) Infiltrated clays in fluvial Jurassic sandstones of Recôncavo basin, Northeastern Brazil. *J. Sed. Petrol.*, **6,** 809–819.

Orr, F.M., Scriven, L.E. and **Rivas, A.P.** (1975) Pendular rings between solids: Meniscus properties and capillary condensation. *J. Fluid. Mech.*, **67,** 723–742.

Pettijohn, F.J., Potter, P.E. and **Siever, R.** (1972) *Sand and Sandstones.* Springer-Verlag, Berlin, 618 pp.

Rao, V.P., Veerayya, M., Nair, R.R., Dupeuble, P.A. and **Lamboy, M.** (1994) Late Quaternary halimeda bioherms and aragonitic fecal pellet-dominated sediments on the carbonate platform of the western continental-shelf of India. *Mar. Geol.*, **121,** 293–315.

Renard, F., Dysthe, D., Feder, J., Bjørlykke, K. and **Jamtveit, B.** (2001) Enhanced pressure solution creep rates induced by clay particles: experimental evidence in salt aggregates. *Geophys. Res. Lett.*, **28,** 1295–1298.

Robson, D.A. (1971) The structure of the Gulf of Suez (Clysmic) rift, with special reference to the eastern side. *J. Geol. Soc.*, **127,** 247–276.

Rose, W. (1958) Volumes and surface areas of pendular rings. *J. Appl. Phys.*, **29,** 687–691.

Said, R. (1962) *The Geology of Egypt.* Elsevier, New York, 377 pp.

Schütz, K.I. (1994) Structure and Stratigraphy of the Gulf of Suez, Egypt. *APPG Mem.*, **59,** 57–96.

Schwarz, T. and **Germann, K.** (1999) *Weathering Surfaces, Laterite-Derived Sediments and Associated Mineral Deposits in North-East Africa. Spec. Publ. Int. Assoc. Sedimentol.*, **27,** 367–390.

Singer, M.J., Southard, R.J., Warrington, D.N. and **Janitzky, P.** (1992) Stability of synthetic sand-clay aggregates after wetting and drying cycles. *Soil Sci. Soc. Am. J.*, **56,** 1843–1848.

Smith, W.O. (1933) The final distribution of retained liquid in an ideal uniform soil. *Physics*, **4,** 425–440.

Walker, T.R. (1976) Diagenetic origin of continental red beds. In: *The Continental Permian in Central, West and South Europe* (Ed. H. Falke), pp. 240–282. Reidel Publishing, Dordrecht.

Wilson, M.D. and **Pittman, E.D.** (1977) Authigenic clays in sandstones: recognition and influence on reservoir properties and paleoenvironmental analysis. *J. Sed. Petrol.*, **47,** 3–31.

Manuscript received 15 October 2002; revision accepted 6 June 2003.